Electrical Double Layer at Various Electrode Potential: A Modification by Vibration

Hualin Zhan,[*,†] Jiri Cervenka,[‡] Steven Prawer,[†] and David J. Garrett[†]

†*School of Physics, The University of Melbourne, Parkville, VIC 3010, Australia*

‡*Institute of Physics ASCR, v.v.i., Cukrovarnická 10/122, 16200 Praha 6, Czech Republic*

E-mail: hualin.zhan@gmail.com

Abstract

This paper proposes a vibration model of ions as an improvement over the conventional Gouy-Chapman-Stern theory, which is used to model the electrical double layer capacitance and to study the ionic dynamics at electrode/electrolyte interfaces. Although the Gouy-Chapman-Stern model is successful for small applied potentials, it fails to explain the observed behaviour at larger potentials, which are becoming increasingly important as materials with high charge injection capacities are developed. By performing a time-dependent study on ionic transport, ions are found to vibrate near the electrode surface, in response to the applied electric field. This vibration allows us to correctly predict the experimentally observed decreasing differential capacitance at high electrode potential. This new model elucidates the mechanism behind the ionic dynamics at solid-electrolyte interfaces, providing useful insight that may be applied to many electrochemical systems in energy storage, photo-electrochemical cells and bio-sensing.

Introduction

Understanding the electrical double layer (EDL) formed at the interface of between a solid electrode and a liquid electrolyte is essential for a wide range of applications, such as supercapacitors, fuel cells, implantable neuromodulation devices and more.[1–4] In essence the EDL is a solid liquid capacitor formed between a solid electrode and dissolved ions in close proximity with a solvent acting as a dielectric. Conventionally, the EDL is modelled using Gouy-Chapman-Stern (GCS) theory.[5] This theory combines the work of Gouy and Chapman with that of Stern who incorporated the earlier work of Helmholtz.

The Gouy-Chapman theory describes a distribution of dissolved ions at a charged surface (diffuse layer) using Maxwell-Boltzmann statistics resulting in an exponential decay of the electric potential into the solution. When the electrode is neutral (point of zero charge, PZC), ions are not attracted or repelled by the surface resulting in electrode surface concentration equivalent to the solution bulk and thus a capacitance minimum. This V-shaped variance of capacitance at moderate electrode voltages, around the PZC, is well predicted. At non-zero electrode voltages the Gouy-Chapman model allows an ion to approach arbitrarily close to the electrode as a size-less point charge, therefore Stern introduced an inner layer (Outer Helmholtz Plane, OHP) with a fixed distance (r_H, defined as Stern layer thickness) adjacent to the electrode surface due to the finite size of the ions.[5] This so-called Stern layer defines a saturation maximum capacitance at high potentials because the capacitance contributed from the Stern layer becomes dominant and the thickness is fixed, as shown in the dashed lines in fig. 1(b). In experiments however, rather than saturating, the EDL capacitance is regularly observed to increase to a maximum and then decrease as electrode potentials move further away from the PZC[6–8] (fig. 1(a)).

The observed decrease of capacitance at high potentials is not predicted by GCS resulting in a large overestimation of electrode capacitance at high voltage. This suggests that the assumption of fixed thickness of the Stern layer may not be correct. The conventional Stern layer has its thickness fixed for only one layer of ions at the electrode surface. This means

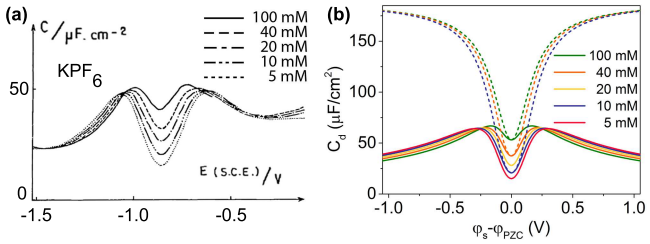

Figure 1: (a) Measured differential capacitance of KPF_6 aqueous solution by silver electrode at different concentration (reprinted from G. Valette, J. Electroanal. Chem., 138, 37 (1982), with permission from Elsevier). (b) Differential capacitance of a KF aqueous solution at different concentration, calculated by the ionic vibration model (solid lines) and by GCS theory (dashed lines).

there is a limit for the areal density of ions on the electrode surface. However, when the actual areal density exceeds the limit created when forming a continuous monolayer, the surplus ions will have to stay on top of the initial "Stern layer", and hence the effective "Stern layer" thickness increases, because only a certain numbers of ions can fit onto the surface. However, the GCS does not take this into account.

Due to the importance of the EDL in various electrochemical systems,[9–23] some attempts have been made to better understand the disagreement between GCS and experimental observations. The most common approach has been to derive a new ionic distribution function using a modified Poisson-Boltzmann equation (mPB)[9–21] or using molecular dynamic simulations.[22,23] An mPB theory accounting for steric effects has been developed by deriving free energy equations from the perspective of statistical mechanics.[9–21] Due to its complex form, however, it is difficult to directly interpret the fundamental physics, such as ionic transport at the interface using this method. Although molecular dynamic simulations are able to provide a better transport picture of complex systems, we attempt a direct analytical approach which provides explicit solutions. Direct study on the dynamic equations, on the other hand, provides explicit solutions and a clearer picture of the ionic transport at the solid-electrolyte interface. However, the sharp peaks in the calculated differential capacitance are not predicted by the mPB theory and not observed in experiments.[17]

In this paper, we present a dynamic model of EDL where, rather than behaving like

stationary solid spheres in the Stern layer, dissolved ions are permitted to react to the charged surface by taking on vibrational energy. Thus at high electrode voltages ionic vibration is larger and the effective Stern layer thickness (r_x) increases. Hence the calculated capacitance, as well as its dependence on potential, is significantly reduced to a value which is comparable to experiment, as shown in fig. 1(b). Similar to Einstein solid,[24] the vibration model suggests that the double layer structure is affected by temperature, this phenomenon is in line with experimental observations.[25]

This model starts with studying a compact Stern layer (layering structure) affected by the steric effect using a concise system of ambipolar diffusion equations (with assumptions which can be relaxed[17]) from which a straightforward solution of effective Stern layer thickness r_x can be obtained. The derived result describes well the decreasing differential capacitance at high electrode potential. This equilibrium theory also predicts sharp peaks at potentials close to PZC. These, however, are not observed in experiments. Therefore, a time-dependent study of ionic transport is performed. This suggests a vibration model[24,26] for the ions where r_x is modified in response to the varying electrode potential. With this change, the modified theory shows very good agreement with experimental results, as shown in figs. 1 and S4. It is worth noting that, similar to the mPB theory,[18] the ionic vibration model also predicts that the differential capacitance (C_d) follows an inverse square root law at higher electrode potential. To simplify the study, the influence of the electrode surface condition, specific adsorption and the difference in ionic radii for anions and cations have been neglected.

Ambipolar diffusion for the steric effects

The total volumetric density of both cations and anions for symmetric electrolyte can be expressed as

$$n_t = n_0 \left(e^{-\frac{ze\varphi}{k_B T}} + e^{\frac{ze\varphi}{k_B T}} \right) = 2n_0 \cosh\left(\frac{ze\varphi}{k_B T} \right), \tag{1}$$

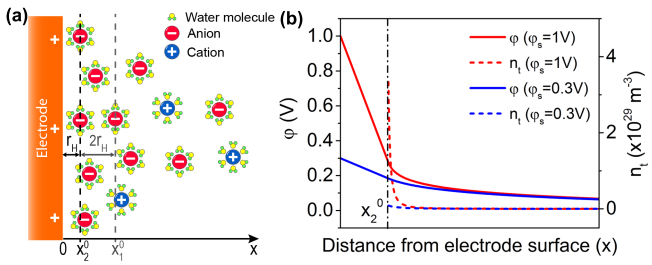

Figure 2: (a) The EDL structure as predicted by GCS theory, where r_H represents the distance from the electrode surface to OHP (located at x_2^0). (b) Potential distribution adjacent to an electrode surface in electrolyte, calculated by GCS theory, where n_t is the total volumetric density of both cations and anions, φ is the local potential at position x in solution, and φ_s is the electrode potential.

where n_0 is the bulk ionic concentration, e is the electron charge, φ is the local potential measured with respect to bulk solution, k_B is the Boltzmann constant, T is the absolute temperature, and z is the charge of cations for symmetric electrolyte[5] (where the charge of anions is $-z$). Integration of n_t from x_2^0 to x_1^0 (as indicated in fig. 2(a)) gives the ionic areal density at the OHP located at x_2^0, $n_{OHP}^{2D} = \int_{x_2^0}^{x_1^0} n_t dx$. The radius of solvated ions is considered the same as the distance from OHP to the electrode surface (the Stern layer thickness, r_H), and $r_H = x_2^0 = \frac{1}{2}(x_1^0 - x_2^0)$. n_{max}^{2D} is defined as the maximal possible local areal density for all ions and molecules in a single ionic/molecular layer. Similar to solid state crystal structures,[27] n_{max}^{2D} can be obtained by arranging ions/molecules in a 2D version of a hexagonal or a centered rectangular lattice, hence $n_{max}^{2D} = (2\sqrt{3}r_H^2)^{-1}$. At a sufficiently high potential, n_{OHP}^{2D} might exceed n_{max}^{2D}, as demonstrated in fig. 2(b). For $\varphi_s = 1V$ in a 10 mM KF electrolyte, a steep increase of n_t is observed near the OHP, resulting in $n_{OHP}^{2D} = 8.4 \times 10^{18} m^{-2}$ (while $n_{max}^{2D} = 2.1 \times 10^{18} m^{-2}$). This, however, is not realistic.

It is then straightforward to presume that the ions stacking on top of the original Stern layer to form a second layer, when the electrode potential is high enough,[15–19] as illustrated in fig. 3(a). These layers (noted as sub-layers in the rest of the paper) comprise a dense region next to the electrode surface, which is called the compact Stern layer. As a result, the location of OHP (x_2) moves away from the electrode surface with the increasing electrode potential (φ_s). Therefore, the effective Stern layer thickness, r_x, becomes greater than r_H,

as shown in fig. 3(a). This in turn affects the differential capacitance.

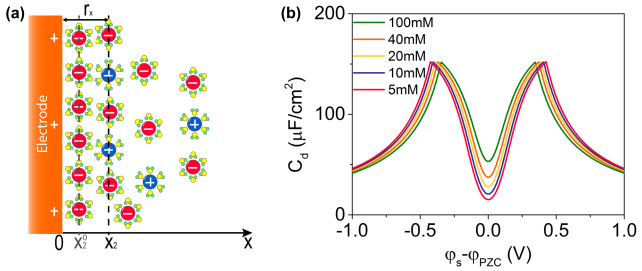

Figure 3: (a) The EDL structure including the compact Stern layer (the layering structure), where r_x, the distance from electrode surface to OHP, increases when the surface concentration reaches the limit. (b) Calculated differential capacitance of KF aqueous solution at different concentration by equation system (2).

It then can be seen that the ions in the compact Stern layer do not follow the simple Boltzmann statics. One approach is to modify the Boltzmann distribution function,[9–21] while another alternative is to study the ion transport using the ambipolar diffusion theory. When the effective Stern layer thickness (r_x) is smaller than the Debye length (λ_D), i.e. $r_x \ll c\lambda_D$ (where $c \sim \sqrt{\varphi_s}$), and $\left|\frac{ze\varphi}{k_BT}\right| \gg 1$, the ambipolar diffusion equations can be written as

$$\begin{pmatrix} \sigma_2 & -\sigma_3 \\ w_2 & w_3 \end{pmatrix} \cdot \begin{pmatrix} E_2 \\ E_3 \end{pmatrix} = \begin{pmatrix} 0 \\ \varphi_s - \varphi_2^{\lim} \end{pmatrix}, \tag{2}$$

where w_2 and w_3, E_2 and E_3, σ_2 and σ_3 are the thicknesses, electric field strengths, and conductivities for sub-layers 2 and 3, respectively. $w_3 = r_H$, $w_2 = r_x - r_H$, and the index 1 is reserved for the diffuse layer. $\varphi_2^{\lim}$ is the potential on new OHP. Note this equation system is only valid at moderate electrode potentials. This is because when the electrode potential is too low ($\left|\frac{ze\varphi}{k_BT}\right| < 1$), there is no compact Stern layer. If the electrode potential is too high, the thickness of the compact Stern layer would exceed the Debye length, i.e. $r_x > c\lambda_D$.

For $\sigma_2 = \sigma_3$ the solution at high potential becomes $E_2 = E_3 = \frac{\varphi_s - \varphi_2^{\lim}}{r_x} = -S^{\lim}$, where $S^{\lim}$ is the slope of $\varphi(x)$ when $x < r_x$. The same result can be obtained numerically,[28] and can also be verified by the mPB theory. This derivation process, the justification for the assumptions, and the complete form of eq.(2) can be found in the supplementary information.

Since the ions distributed away from OHP ($x \in (x_2, \infty)$) still follow Maxwell-Boltzmann statistics, a relation similar to GCS theory can be written $\frac{\varphi_s - \varphi_2^{\lim}}{r_x} = \sqrt{\frac{8n_0 k_B T}{\varepsilon}} \sinh\left(\frac{ze\varphi_2^{\lim}}{2k_B T}\right)$. Hence the differential capacitance is expressed as

$$\frac{1}{C_d} = \frac{r_x}{\varepsilon} + \frac{1}{C_D^{\lim}}, \tag{3}$$

where $C_D^{\lim} = \sqrt{\frac{2\varepsilon z^2 e^2 n_0}{k_B T}} \cosh\left(\frac{ze\varphi_2^{\lim}}{2k_B T}\right)$ is the capacitance of the diffuse layer. It can be proven that $\varphi_2^{\lim}$, hence $S^{\lim}$ and $C_D^{\lim}$ are constant at high electrode potential because the total ionic areal density at OHP is always equal to n_{max}^{2D} when a compact Stern layer is formed. Therefore,

$$r_x = \begin{cases} r_H & (n_{OHP}^{2D} < n_{max}^{2D}) \\ \frac{\varphi_2^{\lim} - \varphi_s}{S^{\lim}} & (n_{OHP}^{2D} = n_{max}^{2D}) \end{cases}. \tag{4}$$

Fig. 3(b) shows the calculated differential capacitance as a function of electrode potential with respect to the PZC using eqs. (3) and (4). The calculated C_d decreases at high potential as observed in the experiments.[6–8] The evident sharp turning points at low potential (around $\pm 0.4V$) have also been predicted in previous reports studying ionic dynamics in compact Stern layer.[17] However these sharp turning points are not observed experimentally, indicating that the theory is inadequate at low potential.

There are two reasons for this. (i) The approximations (e.g. $\frac{ze\varphi}{k_B T} \gg 1$ and $x \ll c\lambda_D$) used to obtain eq. (2) are only valid at moderately high electrode potential. Despite of this, these sharp turning points can still be observed after relaxing these approximations.[17] (ii) Ambipolar diffusion describes the ionic momentum transport at equilibrium where the time-dependent behaviour is neglected.[4,29,30] This mean that the model is suitable for high electrode potential, because the electrostatic force is large. However, the time-dependence should be taken into account at low potential.

Time-dependent study for ionic transport

Similar to most diffusion phenomena investigations,[29–31] a mass transport (or continuous) equation is included in our study. Therefore, a system of equations describing the time-dependent behaviour of the ions near the electrode surface can be written as

$$\frac{\partial n}{\partial t} + \frac{\partial}{\partial x}(nv) = 0, \tag{5a}$$

$$mn\frac{dv}{dt} = mn\left(\frac{\partial v}{\partial t} + v\frac{\partial v}{\partial x}\right) = -\frac{\partial P}{\partial x} + zenE, \tag{5b}$$

$$\frac{\partial E}{\partial x} = \frac{ze\,(n - n_0)}{\varepsilon}, \tag{5c}$$

where P and E are the pressure and the electric field in liquid, m, n and v are the mass, the density and the velocity of the ion, respectively. n_0 is the bulk ionic density at equilibrium. Eqs. (5a) and (5b) are the mass and momentum transport equations, respectively, and eq. (5c) is the Poisson's equation. Although equation system (5) is shown for a single component liquid, the equations and the results for a multi-component solution (a binary system, for example) are very similar. The friction term is also neglected in eq. (5b) for simplicity.

It is convenient to decompose the ionic density into a bulk equilibrium term (n_0, independent on position x and time t) and a perturbation term on electrode surface (n_1, dependent on x and t), i.e., $n = n_0 + n_1$. Rearranging all the equations in equation system (5) and considering the pressure P as a constant in liquid along the direction x, we obtain

$$\frac{\partial^2 n_1}{\partial t^2} + n_1\frac{n_0(ze)^2}{\varepsilon m} = 0. \tag{6}$$

This is a typical harmonic oscillator equation. The perturbation ionic density can be written $n_1 = n_A \exp(-i\omega t)$, where n_A is the amplitude, and the oscillation frequency is $\omega = \pm\sqrt{\frac{n_0(ze)^2}{\varepsilon m}}$. Recall that the oscillation frequency for a harmonic oscillator is $\pm\sqrt{\frac{\eta}{m}}$, we then have $\eta = \frac{n(ze)^2}{\varepsilon}$ as a force constant. This indicates the ionic density near the electrode

surface varies harmonically, while an individual ion vibrates, in response to the electric field. It should also be noted that although the oscillation frequency is only dependent on n_0 and m, the amplitude (and hence the vibration energy) is expected to change with the electric field (potential). This then serves as a basis for our vibration model for ions.

Vibration model for ions

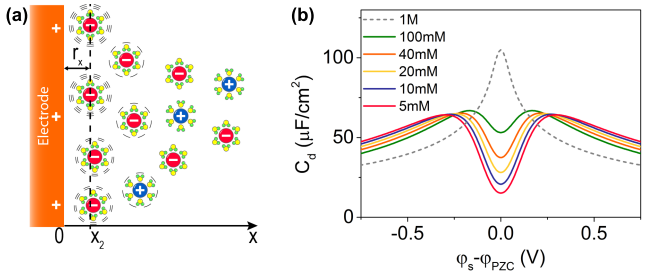

Figure 4: (a), The EDL structure including the vibration model, where r_x, the distance from electrode surface to OHP, increases when the surface concentration reaches the limit. The dashed circles surrounding the solvated ions denote the ionic vibration. (b), Calculated differential capacitance of KF aqueous solution at different concentration by the vibration model.

Vibration models have often been adopted to study inter-molecular forces.[24,26] Our model proposed previously describes short-range ionic interactions, providing a better way to calculate the 'compact Stern layer' thickness. In the presence of electric field, ions will be driven towards the electrode. When they are close enough to the surface, all their potential energy will be converted into kinetic energy and they will bounce back and forth due to Coulombic and short-range intermolecular forces, as shown in fig. 4(a). A real-life analogy is that of dropping a basketball on solid ground. As the object bounces, the general form of the energy conservation equation can be written as

$$\frac{1}{2}n_t\eta(r_x - r_1)^2 + n_t\mathcal{E}_1 = \frac{1}{2}n_t\eta(r_H - r_0)^2 + n_t\mathcal{E}_0 + |n_{net}ze\Delta\varphi|\,, \tag{7}$$

where $n_{net} = n_c - n_a$, η is the force constant, and $\Delta\varphi$ is the potential drop. The left-hand

side in the equation denotes the total ionic energy when the electrode potential $\varphi_s \neq \varphi_{PZC}$, while the first two terms in the right-hand side are the total ionic energy at PZC, and the third term is the electrostatic energy of the ions. $\mathcal{E}_1$ and $\mathcal{E}_0$ are the ionic energies in other forms (for example, the energy exchange due to collision) with and without electric field, respectively. r_x and r_H are the 'compact Stern layer' thicknesses, r_1 and r_0 are the closest distances an ion approaches to the electrode surface, when the electrode is biased at φ_s and φ_{PZC}, respectively. Hence $r_x - r_1$ and $r_H - r_0$ represent the corresponding amplitudes of the vibration. If the electric field does not affect the ionic energy in other forms, i.e. $\mathcal{E}_1 = \mathcal{E}_0$, the solution of r_x is obtained

$$r_x = \sqrt{(r_H - r_0)^2 + \left| \frac{ze}{\eta} \tanh\left(\frac{ze\varphi_x}{k_B T}\right) \Delta\varphi \right|} + r_1, \tag{8}$$

where $\varphi_x = \varphi(r_x)$, $r_1 = r_0$ since $r_x(\Delta\varphi = 0) = r_H$, and a relation $\frac{n_{net}}{n_t} = \frac{n_c - n_a}{n_c + n_a} = \tanh\left(\frac{ze\varphi_x}{k_B T}\right)$ has been used. Since $\Delta\varphi$ increases with the electrode potential, a relation $\Delta\varphi \sim \alpha\varphi_s$ is used to model the differential capacitance in this paper.

Fig. 4(b) shows the calculated capacitance for a KF electrolyte at different bulk concentrations (ranging from 5 mM to 100 mM). It can be seen that the shoulder of the "camel"-shaped curve gets closer to the minimum of PZC compared to the curve depicted in fig. 3(b), or in other words there is an evident decrease in the capacitance value. This is because the OHP gradually moves away from the electrode surface as the ionic vibration becomes stronger at higher potential. The shoulder also gets wider and lower as the bulk electrolyte concentration decreases. The reason is that the diffuse layer capacitance becomes more dominant at lower bulk concentration. All these phenomena have been observed in past experiments as shown in fig. 1(a) and are modelled well by the vibration model.

At high electrode potential, $\tanh\left(\frac{ze\varphi_x}{k_B T}\right) \approx 1$, hence $C_d \sim r_x^{-1} \sim \varphi_s^{-\frac{1}{2}}$. This relation was also confirmed by an mPB theory.[18] The grey dashed line in fig. 4(b) is the differential capacitance for an electrode in a 1 M KF solution. The curve has an interesting "bell"-shape

indicating that the diffuse layer capacitance has only a minor effect on the total differential capacitance. This suggests the vibration model also gives the same prediction as an mPB theory at high surface concentration.[18,21]

It has been experimentally shown that the double layer structure has a temperature dependence.[25] Although a layering structure has been used to model the result, it cannot explain the temperature dependence. Similar to the vibration model for Einstein solids,[24] the presented ionic vibration model suggests that r_x should be dependent on temperature when the ionic energies in other forms are taken into account. This will be included in the future development of the theory.

Conclusion

A modified GCS theory has been developed that enables more accurate modelling of ionic dynamics at solid-electrolyte interfaces. By performing a time-dependent study for ionic transport near the electrode, ions are found to take on vibrational energy from charged surfaces. We demonstrate that the predicted EDL capacitance shows good agreement with experiments, and is also consistent with the modified Poisson-Boltzmann theory including free energy calculations. The reason is that the mass and the momentum transport equations have the same origin as the energy conservation theory in principle, as they are results of the 0^{th}-order, 1^{st}-order and the 2^{nd}-order moment of Boltzmann transport equation, respectively.[30] Please note that the vibration energy also plays a very important role in Marcus charge transfer theory.[26] Therefore this paper may presents a bridge between the EDL capacitance theory and the electron transfer theory, providing an alternative for future development of electrochemical theory.

Acknowledgement

The authors thank the anonymous reviewers for the helpful suggestions. HZ is supported by a Melbourne International Research Scholarship. DJG is supported by Australian Research Council DECRA Grant DE130100922.

Supporting Information Available

The following files are available free of charge.

- Supplementary information: Mathematical details and experimental results.

References

(1) Simon, P.; Gogotsi, Y. Materials for electrochemical capacitors. *Nat Mater* **2008**, *7*, 845–854.

(2) Ito, S.; Zakeeruddin, S. M.; Comte, P.; Liska, P.; Kuang, D.; Grätzel, M. Bifacial dye-sensitized solar cells based on an ionic liquid electrolyte. *Nature Photonics* **2008**, *2*, 693–698.

(3) Armand, M.; Endres, F.; MacFarlane, D. R.; Ohno, H.; Scrosati, B. Ionic-liquid materials for the electrochemical challenges of the future. *Nat Mater* **2009**, *8*, 621–9.

(4) Zhan, H.; Garrett, D. J.; Apollo, N. V.; Ganesan, K.; Lau, D.; Prawer, S.; Cervenka, J. Direct fabrication of 3D graphene on nanoporous anodic alumina by plasma-enhanced chemical vapor deposition. *Sci Rep* **2016**, *6*, 19822.

(5) Bard, A. J.; Faulkner, L. R. *Electrochemical Methods: Fundamentals and Applications*; John Wiley & Sons: New York, USA, 2000.

(6) Valette, G. Double layer on silver single crystal electrodes in contact with electrolytes having anions which are slightly specifically adsorbed Part II. The (100) face. *J. Electroanal. Chem.* **1982**, *138*, 37–54.

(7) Lockett, V.; Sedev, R.; Ralston, J.; Horne, M.; Rodopoulos, T. Differential Capacitance of the Electrical Double Layer in Imidazolium-Based Ionic Liquids: Influence of Potential, Cation Size, and Temperature. *J. Phys. Chem. C* **2008**, *112*, 7486–7495.

(8) Islam, M. M.; Alam, M. T.; Ohsaka, T. Electrical Double-Layer Structure in Ionic Liquids: A Corroboration of the Theoretical Model by Experimental Results. *J. Phys. Chem. C* **2008**, *112*, 16568–16574.

(9) Bikerman, J. J. XXXIX. Structure and capacity of electrical double layer. *The London, Edinburgh, and Dublin Philosophical Magazine and Journal of Science* **1942**, *33*, 384–397.

(10) Gavish, N.; Promislow, K. Systematic interpretation of differential capacitance data. *Physical Review E* **2015**, *92*, 012321.

(11) Stafiej, J.; Ekoka, A.; Borkowska, Z.; Badiali, J. P. New theoretical description of electrified interfaces. *Journal of the Chemical Society, Faraday Transactions* **1996**, *92*, 3677–3682.

(12) di Caprio, D.; Borkowska, Z.; Stafiej, J. Simple extension of the Gouy-Chapman theory including hard sphere effects.: Diffuse layer contribution to the differential capacity curves for the electrode|electrolyte interface. *Journal of Electroanalytical Chemistry* **2003**, *540*, 17–23.

(13) Eigen, M.; Wick, E. The thermodynamics of electrolytes at higher concentration. *J. Phys. Chem.* **1954**, *58*, 702–714.

(14) Borukhov, I.; Andelman, D.; Orland, H. Steric Effects in Electrolytes: A Modified Poisson-Boltzmann Equation. *Phys Rev Lett* **1997**, *79*, 435–438.

(15) Bohinc, K.; Kralj-Iglic, V.; Iglic, A. Thickness of electrical double layer. Effect of ion size. *Electrochimica Acta* **2001**, *46*, 3033–3040.

(16) Bazant, M. Z.; Thornton, K.; Ajdari, A. Diffuse-charge dynamics in electrochemical systems. *Phys Rev E* **2004**, *70*, 021506.

(17) Kilic, M. S.; Bazant, M. Z.; Ajdari, A. Steric effects in the dynamics of electrolytes at large applied voltages. I. Double-layer charging. *Phys Rev E* **2007**, *75*, 021502.

(18) Kornyshev, A. A. Double-Layer in Ionic Liquids: Paradigm Change? *J. Phys. Chem. B* **2007**, *111*, 5545–5557.

(19) Attard, P. Ion condensation in the electric double layer and the corresponding Poisson-Boltzmann effective surface charge. *J. Phys. Chem.* **1995**, *99*, 14174–14181.

(20) Oldham, K. B. A Gouy-Chapman-Stern model of the double layer at a (metal)/(ionic liquid) interface. *J. Electroanal. Chem.* **2008**, *613*, 131–138.

(21) Bazant, M. Z.; Storey, B. D.; Kornyshev, A. A. Double layer in ionic liquids: overscreening versus crowding. *Phys Rev Lett* **2011**, *106*, 046102.

(22) Joly, L.; Ybert, C.; Trizac, E.; Bocquet, L. Hydrodynamics within the electric double layer on slipping surfaces. *Phys Rev Lett* **2004**, *93*, 257805.

(23) Fedorov, M. V.; Kornyshev, A. A. Towards understanding the structure and capacitance of electrical double layer in ionic liquids. *Electrochimica Acta* **2008**, *53*, 6835–6840.

(24) Kittel, C. *Introduction to Solid State Physics*; Wiley, 2004.

(25) Mezger, M.; Schröder, H.; Reichert, H.; Schramm, S.; Okasinski, J. S.; Schöder, S.; Honkimäki, V.; Deutsch, M.; Ocko, B. M.; Ralston, J.; Rohwerder, M.; Stratmann, M.;

Dosch, H. Molecular Layering of Fluorinated Ionic Liquids at a Charged Sapphire (0001) Surface. *Science* **2008**, *322*, 424–428.

(26) Marcus, R. A. On the Theory of Oxidation-Reduction Reactions Involving Electron Transfer. I. *J. Chem. Phys.* **1956**, *24*, 966–978.

(27) Kittel, C. *Introduction to Solid State Physics*; Wiley, 2004.

(28) Burden, R.; Faires, J. *Numerical Analysis*; Cengage Learning, 2010.

(29) Zhan, H. L.; Hu, C. D.; Xie, Y. H.; Wu, B.; Wang, J. F.; Liang, L. Z.; Wei, J. L. Theoretical discussion for electron-density distribution in multicusp ion source. *Applied Physics Letters* **2011**, *98*.

(30) Zhan, H.; Hu, C. Kinetic solutions for electrons in multi-cusp ion source. *Applied Physics Letters* **2011**, *99*, 221501.

(31) Bird, R.; Stewart, W.; Lightfoot, E. *Transport Phenomena*; Wiley, 2007.